1986

Impact Stress Wave Propagation in a Compressor Valve

J. S. Kim

W. Soedell

IMPACT STRESS WAVE PROPAGATION IN A COMPRESSOR VALVE

Jong S. Kim, Ph.D. *

Deputy General Manager,
Daewoo Carrier Corporation
P.O. Box 4803
Syracuse, NY 13221

Werner Soedel

Professor,
Ray W. Herrick Laboratories
School of Mechanical Engrg.
Purdue University,
W. Lafayette, IN 47907

ABSTRACT

This paper is aimed at the fundamental understanding of the impact failure mechanism of the compressor valve plate. The analytical solution of the displacements of the half-space due to a point impact load as a Green's function is derived . The numerical solution of the displacements and stresses in a plate due to the axisymmetric impact pressure are obtained after applying the special convolution and superposition algorithm developed by using the half-space solution. The wave effect on the material failure is clearly demonstrated and the new S-N curve in consideration of the wave propagation due to impact is recommended.

1. INTRODUCTION

There are two types of stresses, bending and impact, associated with a reed valve dynamics. The bending stress develops near the clamped end of a reed as the valve opens and closes. Significant impact stress is generated when the tip or any other portion

* Work was performed while a Graduate Research Assistant at the Ray W. Herrick Laboratories, Purdue University.

of a reed valve strikes its stop or seat with relatively high speed. A simple reed model is shown in Fig. 1.

A fatigue failure may develop near the clamped end or the tip of a reed valve after many operating cycles. Other failures, especially fractures in the vicinity of the valve tip (1), suggest that the contribution of local impact stresses generated by two or three dimensional wave effects may be significant.

As a first step toward the identification and understanding of the impact failure mechanism, the characteristics of the dynamic stress waves in a three dimensional valve reed in the vicinity of the impact force location has been investigated.

It seems impractical to try to obtain the numerical solution from the mathematical formulations for a plate under a point or distributed impact over its surface because of the complex boundary conditions. Therefore, an algorithm called the superposition technique (2) which was used to derive the response of a plate to a line source has been adopted and utilized for this reason. This algorithm and numerical results for a plate are to be presented in Section 4.

Since the relationship between the half-space solution and the plate solution by using the superposition technique has been established, the solution of the half-space should be achieved. Thus, in Section 2, a brief background of the mathematical formulation of a point impact on an elastic half-space and the resultant numerical solutions are presented. The mathematical expression of displacements is represented by complex integral equations. These integral equations are numerically evaluated and presented. Section 3 describes the convolution procedure to distribute a point source over a determined area and some numerical results are presented. The states of stress associated with the displacements for the gate function in half-space are also shown in Section 3. Finally, the discussion and conclusions of the plate solution are to be presented in Sections 5 and 6. The three dimensional results obtained are compared with one dimensional results.

2. POINT IMPACT SOLUTION IN HALF-SPACE

We consider a homogeneous, isotropic and linearly elastic half-space $Z \geq 0$ whose free surface is subjected to a concentrated normal load in Z direction of magnitude. The displacement field is determined from two scalar potentials ϕ and Ψ. Thus, we have to solve the following two scalar wave equations:

$$\nabla^2\Phi = \frac{1}{C_p{}^2}\frac{\partial^2\Phi}{\partial t^2}, \qquad \nabla^2\Psi = \frac{1}{C_s{}^2}\frac{\partial^2\Psi}{\partial t^2}. \qquad (2.1)$$

For the axisymmetric load, the displacements are given as functions of ϕ and Ψ such that

$$U_r = \frac{\partial\Phi}{\partial r} + \frac{\partial^2\Psi}{\partial r\partial z} \qquad (2.2)$$

$$U_z = \frac{\partial\Phi}{\partial z} + \frac{\partial^2\Psi}{\partial z^2} - \frac{1}{C_s^2}\frac{\partial^2\Psi}{\partial t^2}. \qquad (2.3)$$

The boundary conditions at Z = 0 take the form

$$\sigma_z = -f\ H(t)\ \frac{\delta(r)}{2\pi r}, \qquad (2.4)$$

and

$$\sigma_{rz} = 0 \qquad (2.5)$$

where δ and H are delta and Heaviside step function notations, respectively. Thus we have a point impact force applied at the center of the coordinate system with an infinite time dependence. The initial conditions are:

$$\Phi = \frac{\partial\Phi}{\partial t} = 0, \quad \Psi = \frac{\partial\Psi}{\partial t} = 0 \quad \text{at} \quad t = 0. \qquad (2.6)$$

Finally, there is an auxiliary condition that the displacements remain bounded as z goes to infinity. Therefore, our task is to solve the wave equations (2.1) with the boundary conditions in Eqs. (2.4) and (2.5) and the initial conditions in Eq. (2.6) in terms of displacement potentials ϕ and Ψ, and derive an analytical expression for the displacement U_r, U_z after substituting ϕ and Ψ in Eqs. (2.2) and (2.3). For that purpose the Laplace and Hankel transformations are applied. To get the inversion of the transformed equations Cagniard method (3) is to be used. The first author's thesis (4) can be referred to for a detailed mathematical derivation of the final analytical solutions.

The numerical solution of the analytical expression derived was solved by employing the DCADRE routine of the IMSL library on the Cyber 205 super computer system. The vertical displacement of the interior and the surface are shown in Fig. 2 for t=3 micro seconds after the application of a unit point impact force on the surface at the center of the coordinate system. This is marked by an arrow in the figure. Note that the positive U_z denotes downward displacement and the negative U_z denotes upward displacement.

3. NUMERICAL CONVOLUTION

After the displacements due to the point load have been obtained, the displacements due to the distributed impact pressure on the surface of the half-space may be calculated from the convolution procedure in space by superimposing the point load solutions. Thus the point solution can be considered as a Green's function, G_f. If the response G_f at (r, θ) due to a concentrated force at (r', θ') is known, the general response $U(r, \theta)$ due to a distribution of surface impact pressure $p(r, \theta)$ over the contact area, A, can be obtained by superposition:

$$U_j = \int_{r'} \int_{\theta'} p(r',\theta')\, G_f(r-r',\theta-\theta')\, r' dr' d\theta' \qquad (3.1)$$

where

$$dA = r dr d\theta.$$

The response due to an arbitrary time distribution can be calculated in a similar fashion by applying convolution in time. The convolution of this discrete system can be most efficiently performed by applying the FFT (Fast Fourier Transform) algorithm when the given integrand is transformed through the discrete Fourier integral (5). However, this algorithm cannot accurately handle the integrand which changes rapidly and abruptly (6). Furthermore, the integral equation of the Green's function complicates the algorithm. Therefore, a special convolution scheme is desirable. The convolution scheme will fill the contact area by the number of elementary point load and sum the resultant response by using the Green's function concept.

Figure 3 is the typical vertical displacement for arbitrary pressure distribution in space when the time input is given as a gate function. The pressure of unit load is applied on the surface for 1 micro second and then released. The response is taken at t=2 micro seconds after the pressure is released. The surface displacements are not shown because of the Rayleigh singularity in the Green's function. If the load distribution gets more saturated near the center of the R-axis, then the displacement due to that load will monotonically approach the displacement of a point load. We observe that the displacement near the wave fronts has been considerably smoothed out.

The normal and shear stresses are obtained by differentiating the displacement field numerically since the analytical expression for the stresses is quite difficult to derive. Figure 4 illustrates the typical normal stress by the same gate time function input as was used in the displacements. Like the case of displacement, all the static effects are eliminated because of the short time duration of 1 micro second.

4. SUPERPOSITION FOR A PLATE SOLUTION

A plate solution can be obtained by determining the response of every point in a plate over whose surface the impact pressure is applied. Generally, there are three different types of waves propagating through the interior from the point of impact. If we ignore the transmission of waves into the air then all the energy is carried along with the reflected waves leaving a traction free boundary.

The response of a plate is the same as the response of a half-space if the observed time scale is less than the characteristic time of transmission of disturbance across the thickness h, i.e.,

$$t < \frac{h}{C_p} \tag{4.1}$$

where t is the observed time and C_p is the speed of the P wave. However, as soon as the wave front hits the back boundary of the plate, the half-space solution will violate the boundary condition of the plate which is traction free. Since the half-space solution generally has finite stresses other than zero at depth h, artificial stresses must be delivered over the horizontal line of Z=h as shown in Fig. 5 to make the stresses at that line, which correspond to the back surface, zero. The new pressure applied at the surface of the second half-space, which is an overturned form of the original half-space, again, may have finite stresses at Z=h which corresponds to the front surface.

This "calculate and cancel stresses" process will be repeated according to the time frame of interest. The final state of displacements or stresses can be obtained by summing all the responses in each of the half-spaces. This superposition method was used by Shmuely (7) and Blinka (2) for the response of plates to a line source.

However, there is one conceptual difference between the approach in this paper and those of previous researchers. Unlike the case of a line source, there are no analytical solutions of stress available for a point source because of the mathematical difficulties involved in the inversion procedure. This means that we do not have any explicit stress equations to apply as artificial input sources in the superposition process. Thus, a special algorithm needs to be developed in consideration of that difficulty.

Figures 6 and 7 explain two steps of superposition to eliminate the stresses of σ_z and σ_{rz} at the boundaries of a plate to satisfy the boundary conditions. The vertical displacement of the plate is shown in Fig. 8. The pressure is applied again for 1 micro second. The response has been taken at t=2 micro seconds after the pressure is released. The normal and shear stresses are shown in Figs. 9 and 10 for a uniform disk pressure. We can observe stress fluctuation near the S wave fronts. Thus, the material experiences compressive and tensile stresses as the wave propagates and is reflected from the boundary. Based on our experience, it is reasonable to guess that the stress fluctuation at the S wave front would be more severe and abrupt if the pressure distribution were saturated near the center point of the R-axis.

5. DISCUSSIONS AND CONCLUSIONS

It will now be interesting to compare our three dimensional results with the one dimensional results for the displacements and stresses of the plate interior for gate function time dependence as obtained in Section 3. Furthermore, the comparison may serve as a check whether the superposition method has been correctly executed for a plate, since the three dimensional response must approach the one dimensional response if one dimensional loading conditions are imposed.

If the finite pressure distribution is wide enough on a half-space, then the displacement field and the resultant stress field near the surface should be similar to the one dimensional case. Figures 11 and 12 display σ_z for a gate function time dependence for three different cases. In this plot two three dimensional curves have been normalized with respect to a one dimensional curve. Figure 11 shows the response at t=0.58 micro seconds after the application of a gate function pulse of duration time of 1.21 micro seconds. Thus, the leading edge of the pulse has reached the free plate boundary in this time frame. Figure 12 shows the pulse reflection at the free boundary for the same situation. One can clearly observe that the three dimensional solution agrees very well with one dimensional theory when the pressure distribution is wide enough to simulate the one dimensional case. Also, the plot demonstrates the reversal of the stress sign. The compressive pulse reflects as a tensile pulse from the free boundary of the plate, which one dimensional theory has predicted.

Although the valve failure is presumed to result from fatigue type fracture, it would be interesting and instructive to analyze our three dimensional results in terms of material failure such as spalling or scabbing. Figure 13 is a schematic illustration of spalling due to impact on a plate (8). To understand the mechanism by which such spalling occurs, consider the compressive stress pulse traveling through the plate as a result of an impact on the left-hand surface as shown in the figure. As the compressive wave travels through the plate and reaches the free surface, it reflects from the free surface as a tension wave. The reflected tension wave interacts with the incident compressive wave as shown. At a depth h below the right-hand surface of the plate the resultant tensile stress locally exceeds the critical normal fracture stress. The material then fractures, and a scab flies off the surface. Returning to our results shown in Figs. 11 and 12, we have a very similar situation of stress reversal. As the figures show, if the reflected stress wave exceeds the fracture stress of the valve, then a material fracture such as spalling may occur. The phenomenon may increase the stress concentration at the fractured boundary, eventually leading to the catastrophic global fracture. The wave reflection at the locally fractured boundary may contribute greatly to the fracture initiation and propagation. Thus, if the valve material has some defects such as micro cracks or inclusions in its interior, or poor surface finishing, then the wave reflection from the discontinuities might lead to macro cracks. A good surface finishing is believed to have a positive influence on valve failure because the Rayleigh wave is a dominant feature on the surface. Stress wave reflection from the side boundary interacting with the reflected stress waves from the back surface of the plate is also thought to be an important contributing factor to the overall fracture mechanism.

Another point to note about Figs. 11 and 12 is the stress fluctuation. It is well known that a material exhibits surprisingly low critical fracture stress when it experiences stress fluctuation in a repeated loading condition. This stress fluctuation eventually leads to fatigue failure. Since fatigue characteristics of a material cannot be deduced from other mechanical properties, they must be measured directly. Generally this involves laboratory fatigue testing. The rotating-bending fatigue testing machine of the constant bending moment type, for example, is a typical experimental set up used for constructing S-N curves. These curves constitute design information of fundamental importance for machine parts subjected to repeated loading. The S-N curve constructed by this kind of bending-type fatigue test machine is only useful for a harmonic loading condition. As Figs. 11 and 12 imply, the stress fluctuation from compressive to tensile stress or vise versa whenever the traveling wave fronts hit the free boundary of the plate should be considered in generating the S-N curve, because the material undergoes several cycles of stress fluctuation for each impact before the reflected stress wave attenuates due to internal friction. The fatigue stress level in the case of impact is believed far lower than that in the case of sinusoidal loading for this reason. Thus, it is believed that the S-N curve must be constructed from the impact fatigue test machines which incorporate the effect of wave reflection from the free boundary of the plate for a better prediction of valve life. Svenzon (9) made a start in this, but much more work needs to be done. The analysis shown in this paper can be used to interpret controlled fatigue experimental data.

6. CONCLUSIONS

(1) The analytical and numerical solutions of the half-space due to a point impact were obtained.

(2) An efficient numerical convolution algorithm was developed for the response (displacement and stress) of the half-space due to the distributed impact pressure.

(3) The superposition method was developed to obtain the plate response by using the half-space solution.

(4) The importance of the stress reversal and fluctuation in a plate due to the impact stress waves was discussed.

(5) A new impact fatigue test machine was suggested for the better life prediction of a valve.

SYMBOLS

A	contact area
C_p	p wave speed
C_s	s wave speed
f	magnitude of the force
h	thickness of the plate
H	Heaviside step function
R,r	radial position
S	Laplace transformation parameter
t	time
T	normal (T_{zz}) and shear (T_{rz}) stresses
U_r	radial displacement
U_z	vertical displacement
Z,z	vertical position
δ	delta function
∇^2	Laplacian operator
θ	circumferential position
σ	normal (σ_z) and shear (σ_{rz}) stresses
ϕ	scalar displacement potential
ψ	scalar displacement potential

LIST OF REFERENCES

(1) Papastergiou, S., et al., "Impact Velocity of Valve Reeds", Proc. 1982 Purdue Compressor Technology Comference, 1982, pp. 249-256.

(2) Blinka, J., "A Numerical Method for the Analysis of Stress Wave Propagation in Elastic Solids", Ph.D. Thesis, Purdue University, 1984.

(3) Cagniard, L., "Reflection and Refraction of Progressive Seismic Waves", Translated by E.A. Flynn and C.H. Dix, McGraw-Hill Co., 1962.

(4) Kim, Jong S., "Three Dimensional Transient Stress Wave Propagation in a Plate With Application to Compressor Valve Failure Analysis", Ph.D. Thesis, Purdue University, 1986.

(5) Cooley, J.W., Lewis, P.A., and Welch., P.D., "The Fast Fourier Transform Algorithm: Programming Considerations in the Calculation of Sine, Cosine, and Laplace Transforms", J. Sound. Vib., Vol. 12, 1970, pp. 315-337.

(6) Gerald, C.F., and Wheatley, R.O., "Applied Numerical Analysis", Addison-Wesley, 1984.

(7) Schmuely, M., "Stress Wave Propagation in Plates Subjected to a Transient Line Source", Int. J. So. Struc., Vol. 11, 1975, pp. 679-691.

(8) Rinehart, J.S., "Practical Countermeasures for the Prevention of Spallation", Colorado School of Mines, Research Foundation Report AF-SWC-TR-60-7 to Air Force Special Weapons Center, Albuquerque, 1960.

(9) Svenzon, M., "Impact Fatigue of Valve Steel", Proc. 1976 Purdue Compressor Technology Conference, 1976, pp. 65-73.

ACKNOWLEDGEMENTS

Funding for this research project was generously provided by members of the Valve Consortium, consisting of the Copeland Corporation, Mitsubishi Heavy Machines, the Trane Company and the Carlyle Compressor Company. The authors gratefully acknowledge their support.

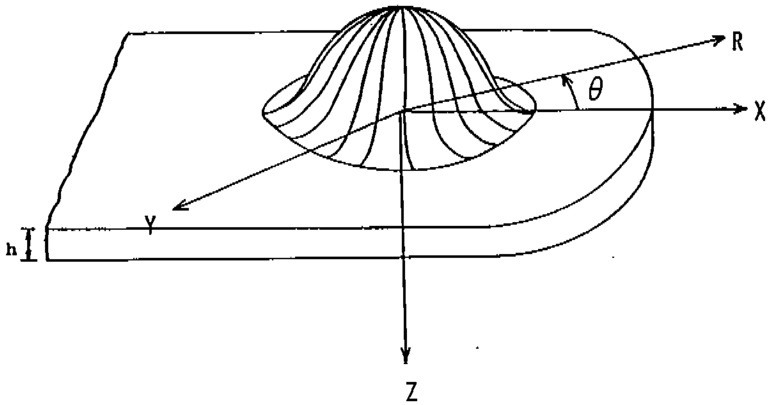

FIGURE 1. Impact pressure distribution on a valve reed model.

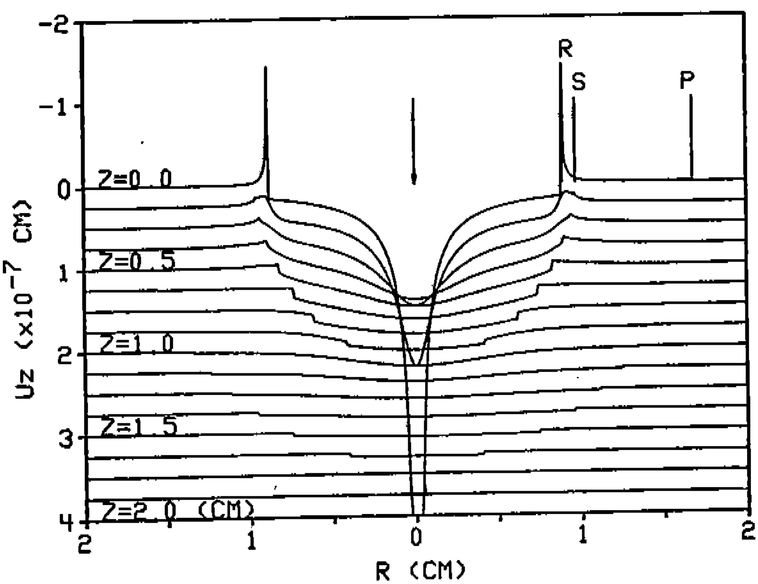

FIGURE 2. U_z vs. R in half-space (point load, Heaviside Fn., t=3 μ sec.)

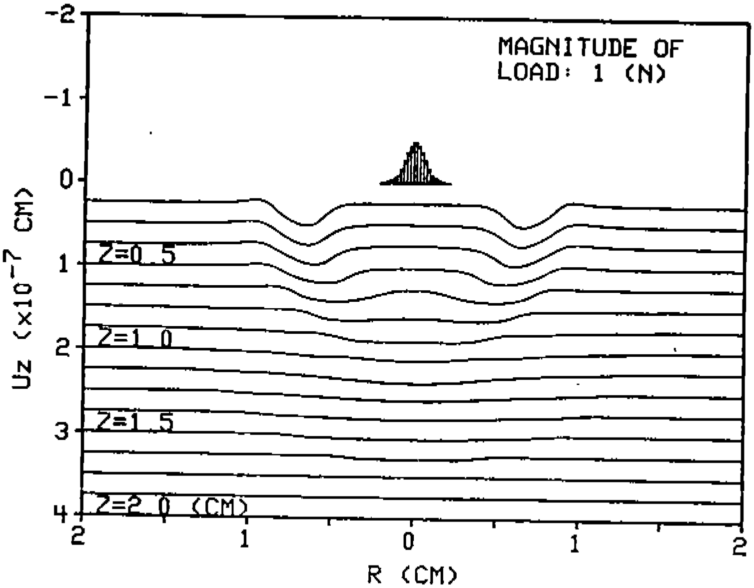

FIGURE 3. U_z vs. R in half-space (Arbitrary pressure distribution, Gate Fn., t=3 μ sec.)

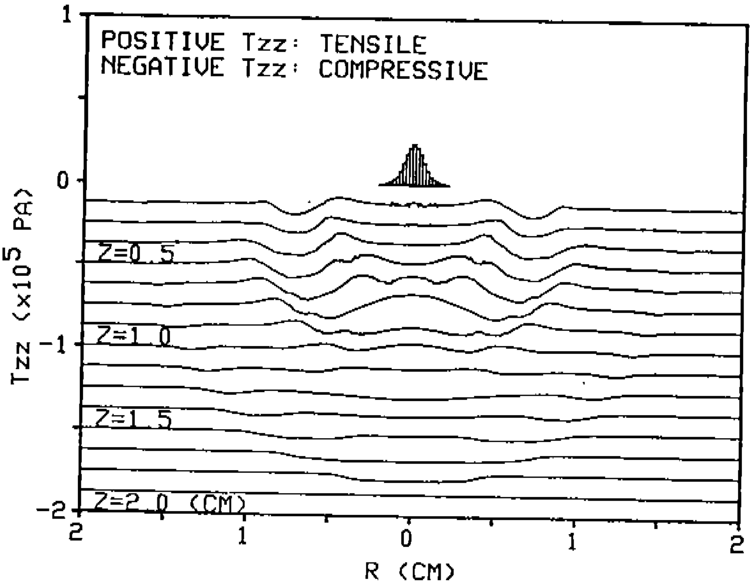

FIGURE 4. σ_z vs. R in half-space (Arbitrary pressure distribution, Gate Fn., t=3 μ sec.)

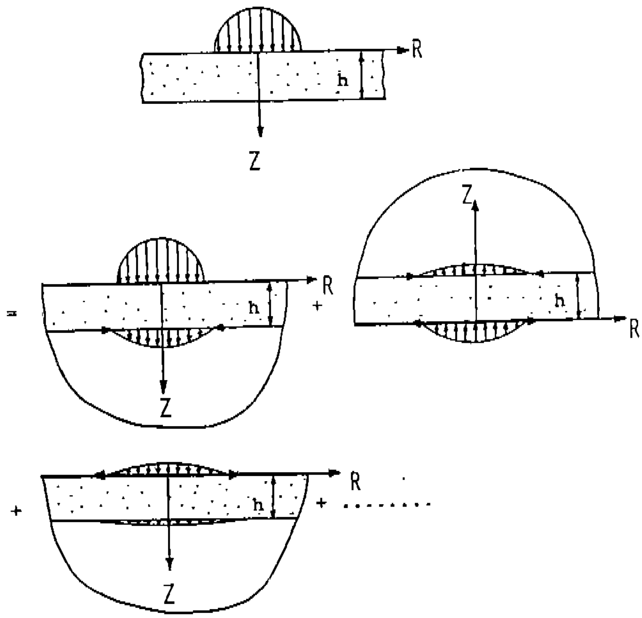

FIGURE 5. Superposition of half-space solutions for the plate solution.

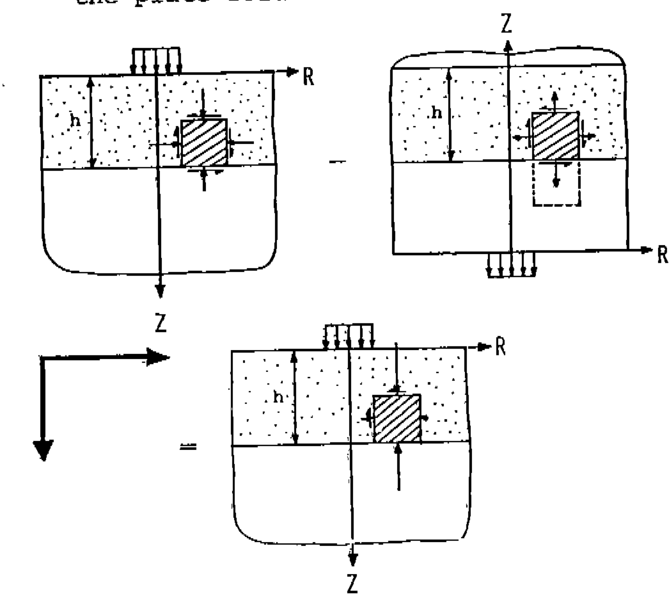

FIGURE 6. First step of superposition to eliminate the shear stress.

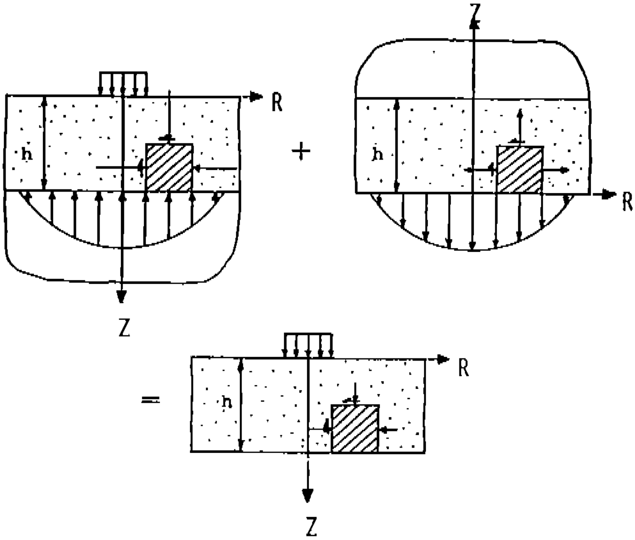

FIGURE 7. Second step of superposition to eliminate the normal stress.

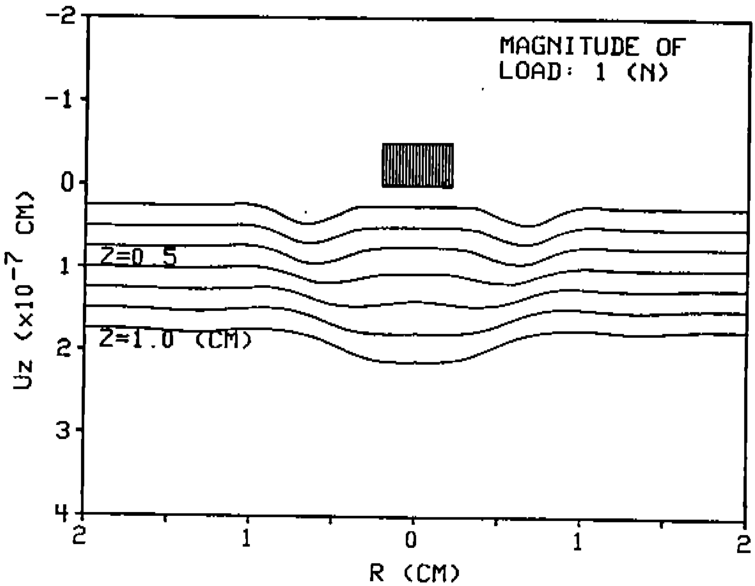

FIGURE 8. U_z vs. R of the plate (Gate Fn., t=3 μ sec.)

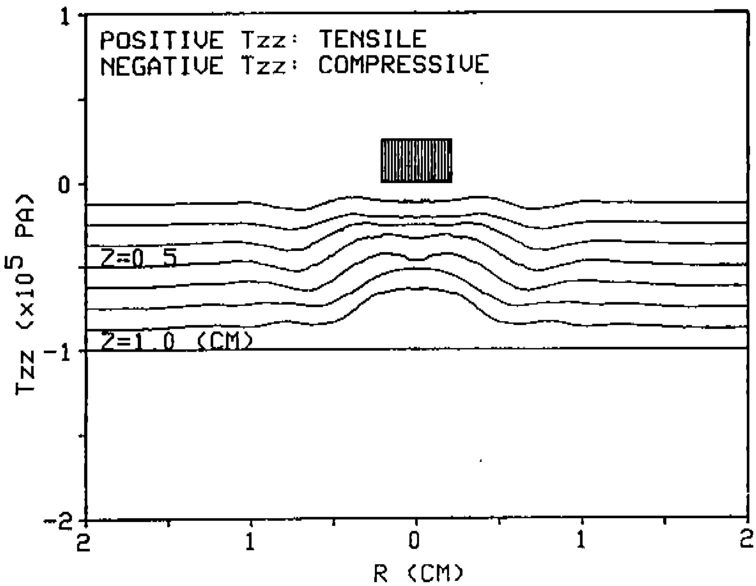

FIGURE 9. σ_z vs. R of the plate (Gate Fn., t=3 μ sec.)

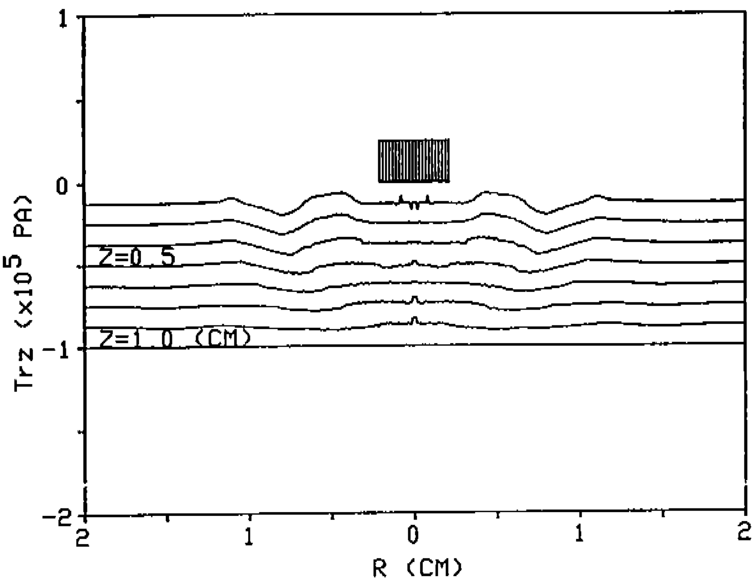

FIGURE 10. σ_{rz} vs. R of the plate (Gate Fn., t=3 μ sec.)

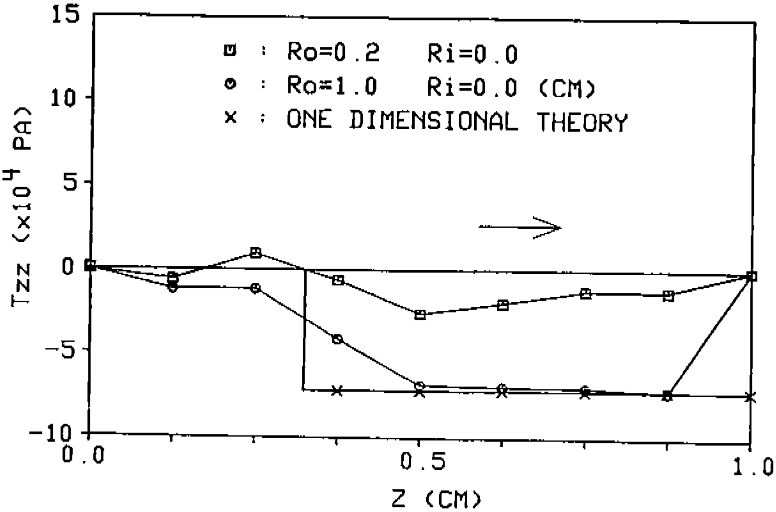

FIGURE 11. Sequential stress wave propagation (Gate Fn., t=1.21 μ sec.)

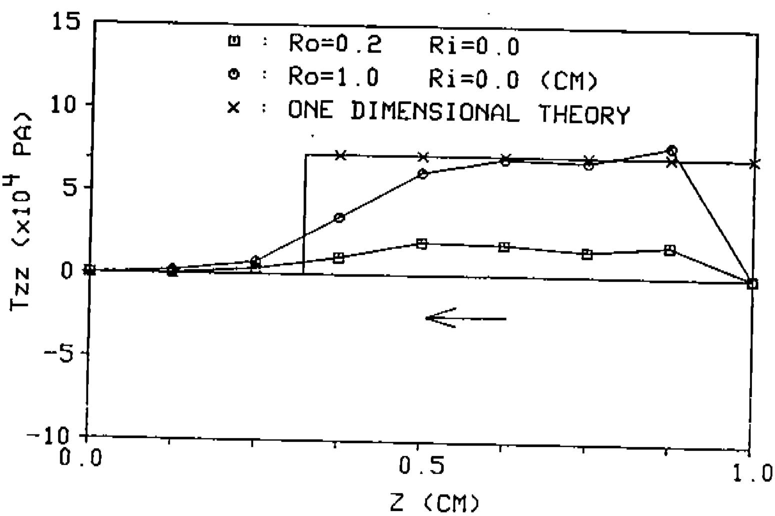

FIGURE 12. Sequential stress wave propagation (Gate Fn., t=3.0 μ sec.)

SELF-EXCITED VIBRATIONS OF RECIPROCATING COMPRESSOR PLATE VALVES

S. Ziada, S.J. Shine, and E.T. Bühlmann

Laboratory for Vibrations and Acoustics,
Sulzer Brothers Limited,
Winterthur, Switzerland

ABSTRACT

The self-excitation mechanism causing the flutter of reciprocating compressor plate valves is experimentally investigated under steady state conditions. The relation between the plate oscillations and the resulting pressure pulsations is established by means of simultaneous recording of the plate movements and the upstream and downstream pressure pulsations.

It is shown that movements of the valve plate produce fluid forces which are destabilizing because they are in phase with the velocity of the plate. Thus, acoustic resonances of the piping system are strongly excited due to their coupling with the vibration of the valve plate. The stiffness of the valve springs has been found to have very little influence on the vibration frequency which is controlled by the system acoustical resonances.

Whilst the system oscillation is sustained, the valve plate stays parallel to the seat, but substantial plate tilting eliminates this vibration. Thus, the valve vibrations can be eliminated by using unevenly distributed springs which force the valve plate to tilt while opening.

1. INTRODUCTION

Self-excited vibrations of spring loaded compressor valves are sustained via a destabilizing fluid force which increases as the valve lift is increased. Several investigations have characterized experimentally (1, 2) and theoretically (3, 4) this destabilizing fluid force as a force (or a pressure) coefficient